

# Postmortem Raman Spectroscopy Explaining Friction and Wear Behavior of Sintered Polyimide at High Temperature

P. Samyn, J. Van Craenenbroeck, F. Verpoort, and P. De Baets

(Submitted March 16, 2006; in revised form April 4, 2006)

With their thermal stability and high strength, polyimides are an aromatic type of polymers that are used in sliding equipment functioning under high loads and elevated temperatures. However, their tribological behaviors under high temperature and atmospheric conditions are not fully understood. It has been reported that a transition from high to lower friction occurs “somewhere” between 100 and 200 °C; however, correlation with changes in the polyimide molecular structure remains difficult to illustrate, and it is not certain whether this transition is correlated to lower wear. In the present work, sliding experiments under controlled bulk temperatures between 100 and 260 °C are performed. A transition in both friction and wear at 180 °C is observed that is further examined with microscopic analysis of the transfer film on the steel counterface and Raman spectroscopy of the worn polymer surfaces. Close examination of the spectra reveals transitions in the relative intensities of certain absorption bands, which suggests different orientation effects of the molecular conformation at the polymer sliding surface at 180 °C.

**Keywords** friction, polyimide, Raman spectroscopy, temperature, wear

## 1. Introduction

The favorable use of polymer materials in dry sliding is indicated by their self-lubricating ability with limited material transfer from the one rubbing surface to the other, which is induced by viscous flow of the polymer part. However, the practical application range of most technical polymers as, e.g., polyamides, polyacetals, or polyethylene terephthalate is limited due to their low thermal stability. The temperature generated during friction causes weakening and melting that result in loss of mechanical strength and load-carrying capacity. Polyimides possess an extremely high thermal resistance and are therefore used in high-performance sliding applications, where superior mechanical, chemical, and thermal properties are required (e.g., in high-load-bearing applications). The maximum short- and long-term temperature exposures of most commonly used technical polymers are shown in Fig. 1 (Ref 1). Pioneering research on the tribological behavior of polyimides and its self-lubricating ability in film or bulk material has been performed by Fusaro (Ref 2) and Tewari and Bijwe (Ref 3), mainly under vacuum conditions used for space applications. Although their studies show transitions in friction and wear mechanisms at higher sliding temperatures, the reasons behind these observations remain difficult to illustrate and become

P. Samyn and P. De Baets, Ghent University, Laboratory Soete, Department of Mechanical Construction and Production, Sint-Pietersnieuwstraat 41, B-9000 Gent, Belgium; and J. Van Craenenbroeck and F. Verpoort, Ghent University, Laboratory of Organometallics and Catalysis, Department of Inorganic and Physical Chemistry, Krijgslaan 281 (S3), B-9000 Gent, Belgium. Contact e-mail: Pieter.Samyn@UGent.be.

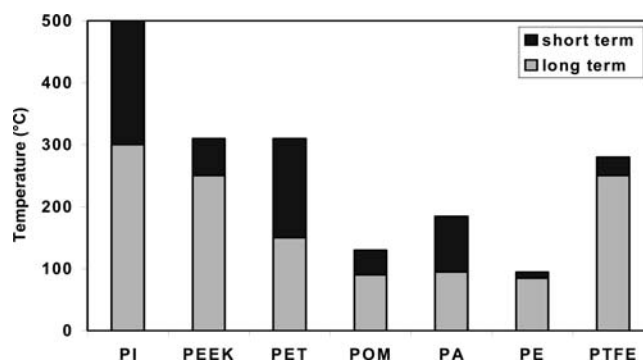
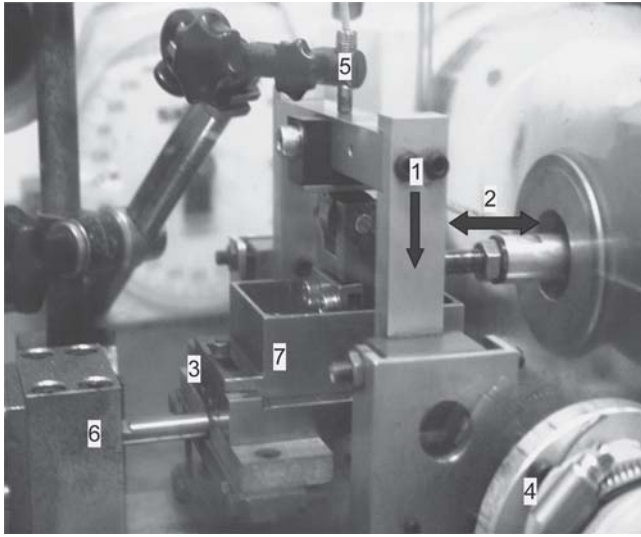


Fig. 1 Thermal stability of polyimide relative to other frequently used technical polymers [temperatures for short and long exposures in, e.g., bearing applications (Ref 1)]

more pronounced under atmospheric sliding conditions. It is believed that close examination of the polyimide transfer behavior (Ref 4) and the worn polymer surfaces will provide additional information related to changes in the material's physical or chemical structure under sliding (Ref 5). In-depth analyses of the variation in the polyimide structure during sliding have rarely been investigated by means of Raman spectroscopy (Ref 6). This rapid and nondestructive technique allows measurement of molecular vibration and rotational energy changes. The requirement for vibrational activity in Raman spectra is not a change in dipole moment, as in infrared (IR) spectra, but rather a change in the polarizability of the molecule. The phenomenon of inelastic light scattering of a laser-irradiated surface is known as Raman radiation: when a substance is irradiated with monochromatic light, most of the scattered energy comprises radiation of the incident frequency (Rayleigh scattering). In addition, a very small quantity (0.0001%) of photons with shifted frequency is observed. The fraction of photons scattered from molecular centers with less



**Fig. 2** Reciprocating cylinder-on-plate tribotester, test parameters: (1) normal load, (2) reciprocating sliding velocity, (3) resistance heating, and (4) climate conditioner measurements: (5) vertical displacement, (6) friction force, and (7) bulk temperature

energy than they had before the interaction is called Stokes scattering. The anti-Stokes photons have higher energy than those of the exciting radiation. The frequency of the scattered radiation is characteristic for both the composition and the orientation of a molecular structure.

## 2. Experimental Procedures

### 2.1 Tribological Test Set-Up and Test Parameters

Friction and wear tests are done on a cylinder-on-plate configuration in a PLINT TE 77 (Phoenix Tribology Ltd., Whitway, Newbury, UK) reciprocating test rig (Fig. 2). A line contact between the polyimide cylinder (diameter, 6 mm; length, 15 mm) and the fixed steel counterface is applied. The initial contact is said to be counterformal, although it continuously grows as wear proceeds, which is referred to as an “increasing contact area” type of wear. A piezo-electrical force transducer is used to measure the horizontal frictional force. The normal displacement of the cylinder toward its counterface is continuously measured by a contactless proximitor. Sliding temperatures are measured by a DIN 43,710 K-type (Phoenix Tribology Ltd., Whitway, Newbury, UK) (nickel-chromium/nickel-aluminum) thermocouple positioned on top of the steel counterface, representing the average bulk temperature.

The oscillating motion of the polymer sample is provided by a controlled variable-speed motor through an eccentric power transmission for adjustment of the stroke (15 mm). The sliding frequency is fixed at 10 Hz, corresponding to a sliding velocity of 0.3 m/s. The total sliding distance comprises 15 km if no overload situation occurs, corresponding to a sliding time of 13.5 h. The normal load  $F_N$  is applied by a bridge that is mechanically pulled down by rotation of a crank handle. The normal force is transmitted directly onto the moving specimen by means of a roller cam. Different normal loads  $F_N$  of 50, 100, 150, and 200 N are applied corresponding with initial contact situations as given in Table 1. The initial contact pressure is calculated according to the Hertzian law in Eq 1 for the peak ( $p_H$ ) and mean ( $p_{\text{mean}}$ ) contact pressures, respectively:

$$p_H = \sqrt{\frac{(F_N/b)E}{2\pi R}} \quad p_{\text{mean}} = \frac{\pi}{4} p_H \quad (\text{Eq 1})$$

where  $b$  is the width of wear track (15 mm) and  $R$  is the cylinder radius (3 mm). From those parameters, the initial contact area  $A_S$  and elastic indentation  $\delta_H$  is calculated. The steady-state contact pressure is geometrically calculated from the wear depth  $\Delta h$  (measured on the worn specimen by means of a micrometer) according to Eq 2 with  $\ell$  the semilength of the contact area in the sliding direction.

$$p = \frac{F_N}{A} = \frac{F_N}{b \, 2\ell} = \frac{F_N}{b \, 2\sqrt{R^2 - (R-h)^2}} \quad (\text{Eq 2})$$

The contact temperature is artificially applied through constantly heating the steel counterface at 100, 140, 180, 220, and 260 °C. The heat is generated by electrical resistance under the plate holder and is regulated by a proportional-integral-derivative (PID) controller. As those temperatures represent an average temperature over the entire sliding surface, they are further referred to as “bulk temperatures.” The relative humidity is controlled at 60% for all tests by means of a climate box surrounding the contact zone.

### 2.2 Fourier Transform Raman Spectroscopy

Measurements of Raman spectra on the worn polyimide surfaces are performed on a Bruker FT spectrometer Equinox 55S (Bruker Optik, Ettlingen, Germany), equipped with a Raman module FRA 106 that is fitted to a nitrogen-cooled (77 K) germanium high-sensitivity detector D418-T. The applied laser wavelength during the experiments is the 1.064  $\mu\text{m}$  line from a diode laser pumped Nd:YAG laser. All spectra are recorded at a resolution of 3  $\text{cm}^{-1}$  using a nonfocused laser beam with a power of 70 mW. Each spectrum is collected as an average of 250 scans, where the applied parameters result in a clear spectrum for all test samples. Divergence of the spectrum over different points on the sliding surface is small. Data collection and data transfer are automated using Bruker OPUS software. The spectra are studied in the absorption band range between 500 and 2000  $\text{cm}^{-1}$ .

### 2.3 Test Material

Sintered polyimide Vespel SP-1 is used as an unfilled base resin in current tribological research. Its mechanical and physical properties are listed in Table 2 (Ref 7). The imide functional group provides the polymer extremely high mechanical properties and stability. Sintering the polyimides after chemical reaction provides semithermosetting characteristics. As such, no transition temperature has been revealed and the mechanical properties decrease linearly with higher temperatures only slightly, in contrast with other thermoplastics (as shown in Fig. 3) (Ref 8). The counterface plates are made of hardened and tempered 40 CrMnNiMo8 steel (DIN 1.2738) with hardness of 300 HB and surface roughness  $R_a = 0.10 \mu\text{m}$ . The roughness is chosen to be relatively low because it has been reported that polyimides do not perform well under abrasive conditions (Ref 9). Presently, adhesion will be the most important mechanism of wear.

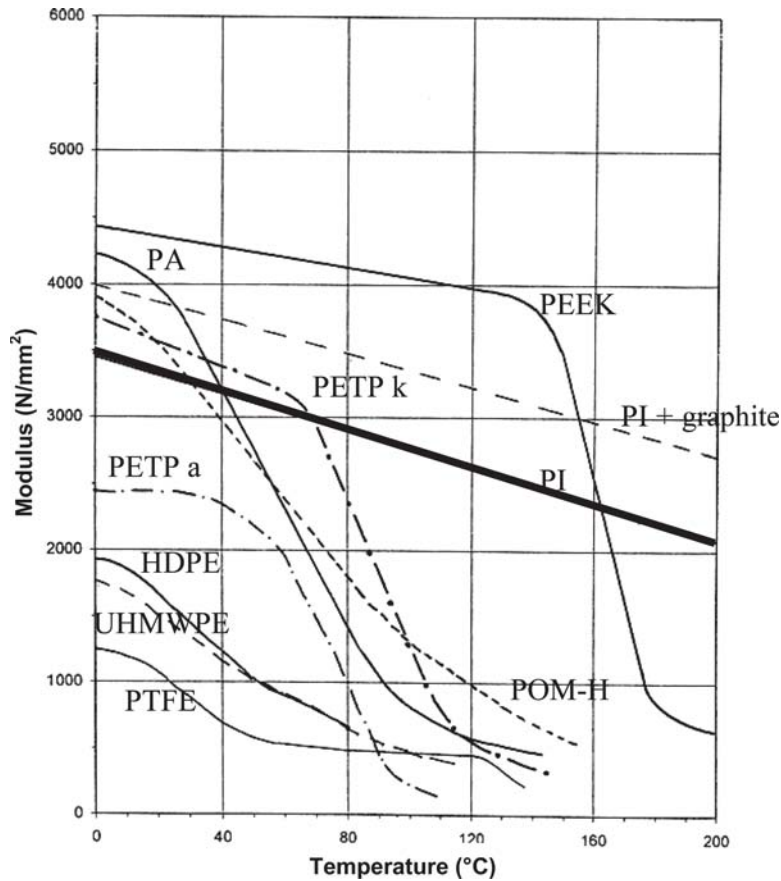


Fig. 3 Mechanical properties of polyimide as a function of temperature (Ref 8)

Table 1 Contact conditions for initial line contact and steady-state contact at end of the sliding test

| $F_N$ , N | Initial Hertz line contact |                   |                         |                      | Steady-state contact ( $v = 0.3$ m/s) |                 |                 |                 |
|-----------|----------------------------|-------------------|-------------------------|----------------------|---------------------------------------|-----------------|-----------------|-----------------|
|           | $p_{H,avg}$ , MPa          | $p_{H,max}$ , MPa | $A_s$ , mm <sup>2</sup> | $\delta_H$ , $\mu$ m | 100 °C                                | 140 °C          | 180 °C          | 260 °C          |
|           |                            |                   |                         |                      | $p_{avg}$ , MPa                       | $p_{avg}$ , MPa | $p_{avg}$ , MPa | $p_{avg}$ , MPa |
| 50        | 30                         | 38                | 1.7                     | 2.5                  | 0.96                                  | 0.95            | 0.93            | 0.89            |
| 100       | 43                         | 54                | 2.3                     | 4.6                  | 1.73                                  | 1.92            | 1.63            | 1.49            |
| 150       | 52                         | 67                | 2.8                     | 6.6                  | 2.19                                  | 3.82            | 2.68            | 2.33            |
| 200       | 61                         | 77                | 3.3                     | 8.5                  | 2.94                                  | 2.92            | 2.98            | 3.04            |

Table 2 Physical and mechanical properties of sintered polyimides

|                          | Tensile strength, MPa | Elongation, % | Flexural strength, MPa | Elasticity modulus, MPa | Compressive strength, MPa |            | Thermal conductivity, W/m °C |
|--------------------------|-----------------------|---------------|------------------------|-------------------------|---------------------------|------------|------------------------------|
|                          |                       |               |                        |                         | 1% strain                 | 10% strain |                              |
| SP-1 polyimide at 23 °C  | 72                    | 7.5           | 82.7                   | 2480                    | 24.1                      | 112.4      | 0.29                         |
| SP-1 polyimide at 260 °C | 36.5                  | 7             | 44.8                   | 1448                    | ...                       | ...        | ...                          |

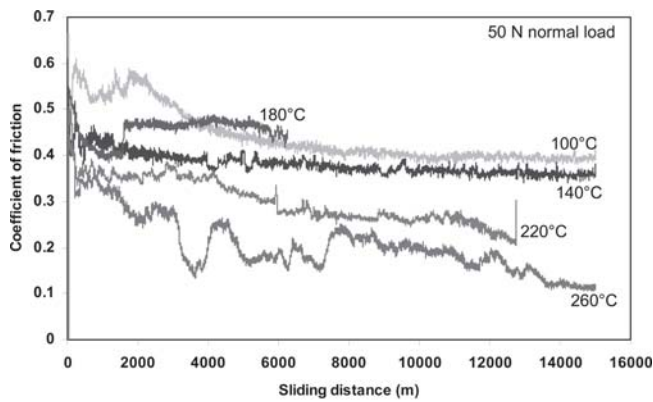
Source: Ref 7

### 3. Test Results

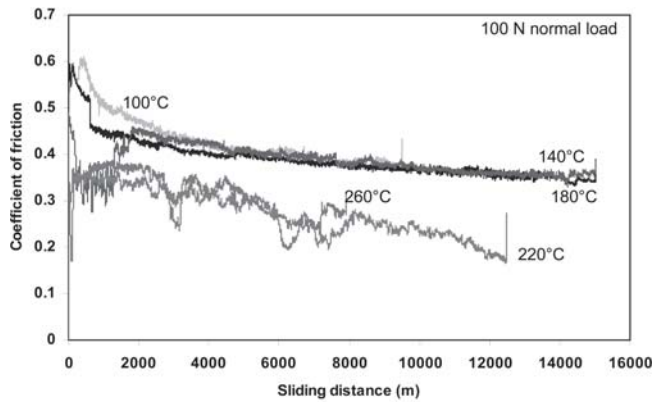
#### 3.1 Friction

For the sliding tests at 50 and 100 N normal loads, the coefficient of friction is recorded as a function of the sliding distance in Fig. 4. It is observed that running-in effects cause

strong variations in friction and that friction decreases progressively with increasing sliding distance toward a more or less stable steady-state value that is attained after approximately 4000 m of sliding. The running-in effects are attributed to a combined effect of deformation at the initial line contact and orientation of the polymer chains at the sliding surface. The



(a)



(b)

**Fig. 4** Coefficient of friction continuously measured as a function of sliding distance for different bulk temperatures under normal loads of (a) 50 and (b) 100 N

increase in bulk temperature causes a decrease in friction, although less stable friction is attained. Stabilization in friction occurs more difficult at higher sliding temperatures. Those instabilities result from the progressive build-up and removal of a transfer layer onto the steel counterface, as discussed later on.

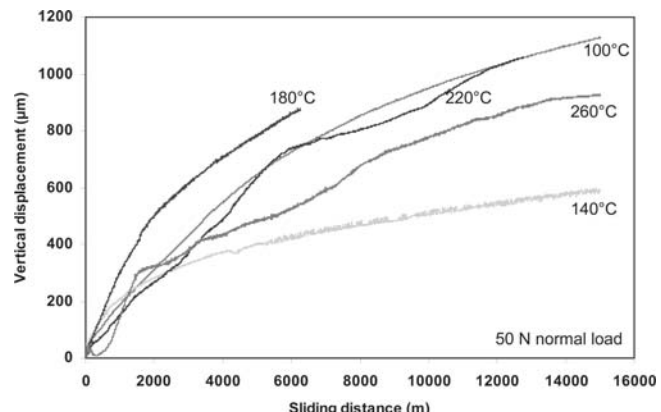
### 3.2 Wear

The wear of the polyimide cylinders is continuously recorded as the vertical displacement of the polymer cylinder toward its mating plate. Under normal loads of both 50 and 100 N, the wear curves are plotted as a function of sliding distance (Fig. 5). Most of the small-scale tests under controlled temperature show a linearly increasing wear depth with the sliding distance; only at temperatures above 180 °C is a clear separation between running-in and steady-state wear observed. After a certain period of increasing wear depth at high wear rate, it decreases slightly toward a slower steady-state increase in wear. At higher temperatures (i.e., 220 and 260 °C), the vertical displacement curve is less stable, as the transfer of polymer parts into the contact interface and their plastification destabilize both friction and wear measurements.

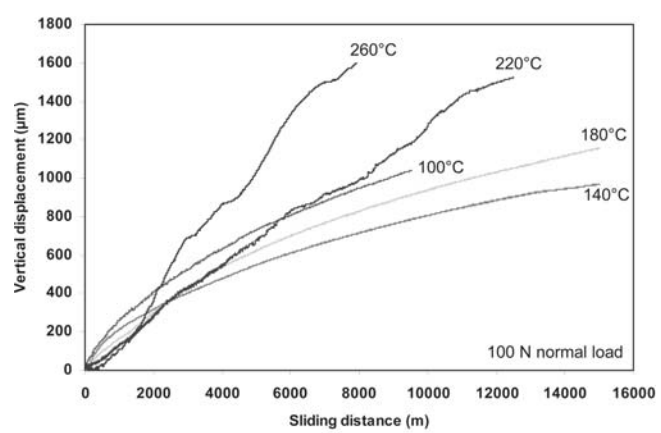
## 4. Discussion

### 4.1 Influence of Temperature on Friction and Wear

A plot of the coefficients of friction as a function of temperature for different normal loads between 50 and 200 N is



(a)

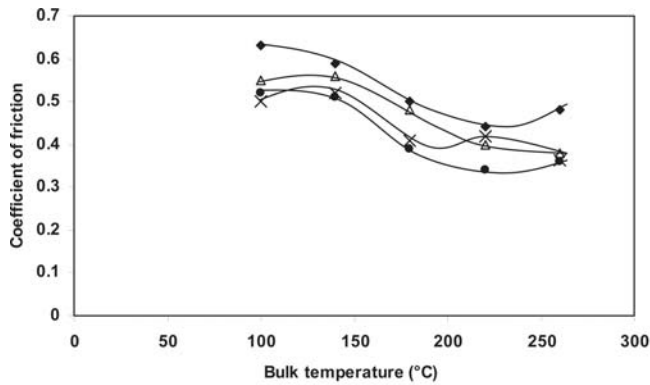


(b)

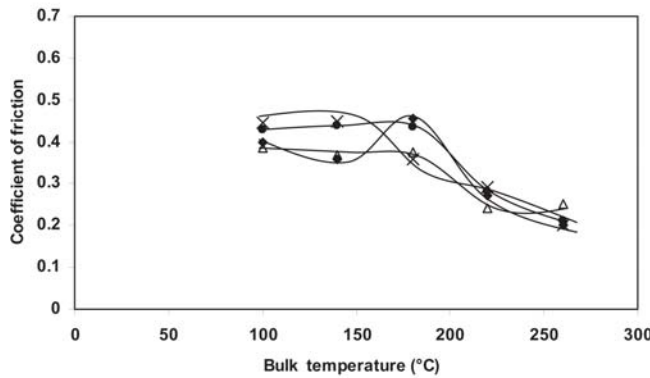
**Fig. 5** Vertical displacement continuously measured as a function of sliding distance for different bulk temperatures under normal loads of (a) 50 and (b) 100 N

shown in Fig. 6. They represent an average value calculated at the beginning (after 100 m) and at the midpoint of the sliding test (8000 m). As a function of temperature, a transition in friction from 180 °C on is found for each of the applied normal loads. Even at low sliding distances, this trend is observed, but it becomes the most evident at the end of the sliding test. At lower temperatures, friction is either constant or increases little, but it decreases abruptly at a higher temperature. At low loads (50 N), friction decreases progressively as a function of temperature, but a characteristic peak in friction toward a maximum value of 0.48 is found at 180 °C.

The polyimide volumetric wear rates are calculated from weight measurements before and after testing (Fig. 7). Although weight measurements are the most effective for the real material loss, dimensional changes would include also information on deformation and creep. Therefore, the continuous measured curves of vertical displacement as described previously are characteristic for both wear (as material loss) and deformation (creep and thermal expansion). The data reported herein pertain to the wear rates (material loss) calculated over the entire test period, including both the running-in period and steady-state conditions. It is clear that higher bulk temperatures do not certainly imply higher wear rates of polyimides, as is generally expected for thermoplastic polymers. At low loads, stabilization in wear rates occurs even under higher bulk temperatures. The observed peak in wear rate under a normal load



(a)



(b)

**Fig. 6** Effect of bulk temperature on friction after (a) 100 m and (b) 8000 m of sliding, for normal loads of (◆) 50, (△) 100, (●) 150, and (×) 200 N

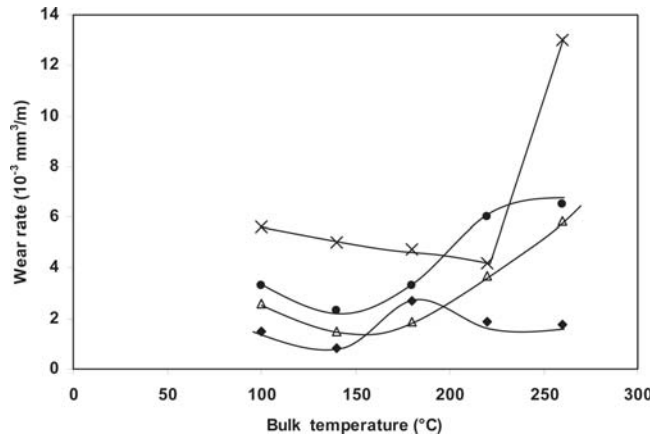


**Fig. 7** Effect of bulk temperature on volumetric wear rates for normal loads of (◆) 50, (△) 100, (●) 150, and (×) 200 N

of 50 N and bulk temperature of 180 °C is in accordance with the previously observed characteristic peak value in friction. At higher loads (100 to 200 N), decreasing wear rates between 100 and 140 °C are measured. However, when the bulk temperatures rise above 180 °C overload situations occur, leading to a sudden increase in wear rates.

Tewari and Bijwe (Ref 3) also observed a peak in the steady-state friction and wear, but with the position of the transition peaks depending on the sliding speed. Although the friction peak occurred at 150 °C, it seems not uniquely corre-

lated to the wear peak that occurred at 200 °C. In the experiments run for this study, both friction and wear peaks under a 50 N normal load seem to be better correlated to each other. Matsubara et al. (Ref 10) explained the occurrence of a peak value as an interaction between the increase in abrasive action and the chemical changes of the polyimide with increasing temperature. The first observations of a transition in the polyimide friction and/or wear were reported by Fusaro (Ref 11) by investigating the effect of moisture in air on the tribological properties of a polyimide film. He showed that the transition temperature, at which the coefficient of friction decreased, increased in moist air and the coefficient of friction at temperatures below the transition temperature was lower in moist air with greater wear at high temperatures in moist air. The transition was found to occur in inert atmosphere (dry argon, <20 ppm H<sub>2</sub>O) or in dry air (<20 ppm H<sub>2</sub>O) at 40 ± 10 °C). When water vapor was present in the air (10,000 ppm H<sub>2</sub>O), the transition was prevented or shifted upward to be between 100 and 200 °C. Due to observation of influences of environmental atmosphere on friction and wear, the transitions were attributed to the higher polymer-chain mobility and enhanced molecular orientation at the surface in absence of water, leading to a texture conducive to easy shear. Such a texture could be produced by an extended chain molecular structure with the chains tilting or stretching parallel to the sliding direction. In parallel, the increase in bulk temperature between 100 and 200 °C at the sliding interface in present tests are able to break the hydrogen bonds and to reduce the absorbed moisture by liberating water. From that moment on, molecular reorganization becomes possible and results in lower friction. At temperatures below the transition, this reordering cannot occur because the molecules do not possess the degree of freedom necessary for rotation.

#### 4.2 Polyimide Transfer onto the Steel Counterface

The wear tracks on the steel counterface are evaluated by optical microscopy after the sliding tests. Figure 8 shows the different features of the sliding counterfaces as a function of normal load and applied bulk temperature. At low temperatures (100 to 140 °C), there is no evidence of any transfer film. Close examination of the counterface only reveals some depositions of separate wear debris into the surface grooves. This is in accordance with the generally accepted orientation theories because high stiffness and low weakening prevent the polymer chains from being oriented and being drawn out of the surface. Only higher temperatures from 220 to 260 °C cause formation of transfer films by partial plastification of the polymer sliding surface and the transferred wear debris. Although the transfer film becomes more homogeneously spread and thinner at higher loads and/or bulk temperatures, in none of the cases was an entirely smoothed and homogeneous film observed, possibly because of the rather brittle characteristics of polyimide, which prevent entire elongation and drawing out of the polymer chains from the surface. Formation of a plastified transfer layer onto the steel surface at higher temperature may cause the presently observed transitions from high friction at low temperature to low friction at high temperature, with the transition characteristically manifesting at 180 °C. Also, the separation between high running-in wear (Fig. 5) and lower steady-state wear is caused by the progressive transfer during sliding.

The change in morphology of the wear surface reflects a change in friction and wear mechanisms as a function of the

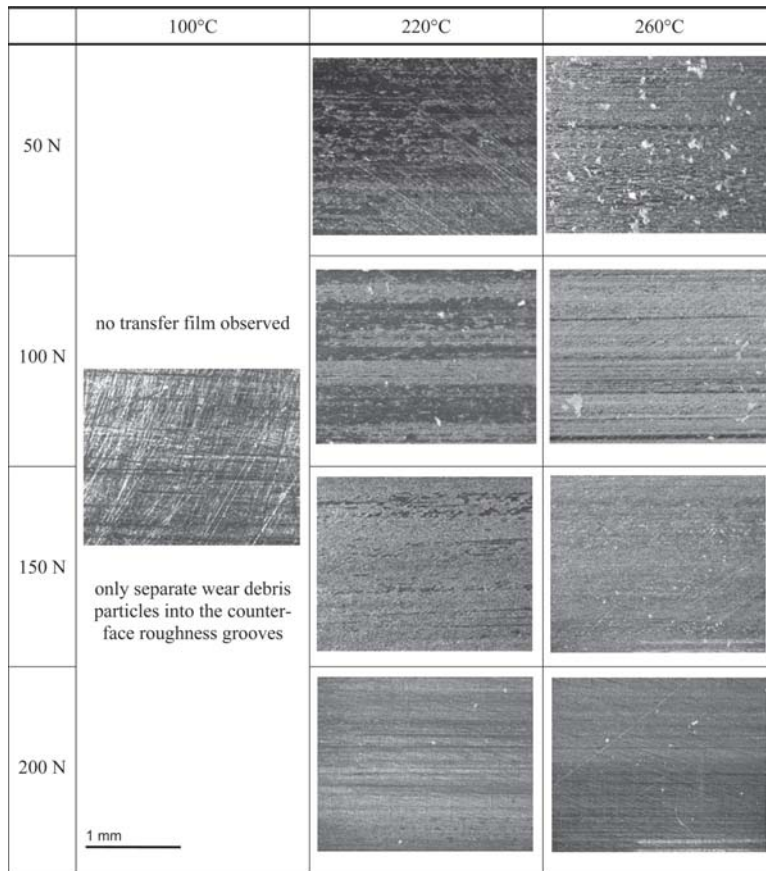


**Fig. 8** Optical microscopy of the polyimide transfer on steel counterfaces at bulk temperatures of 100 (no transfer), 220, and 260 °C under different normal loads

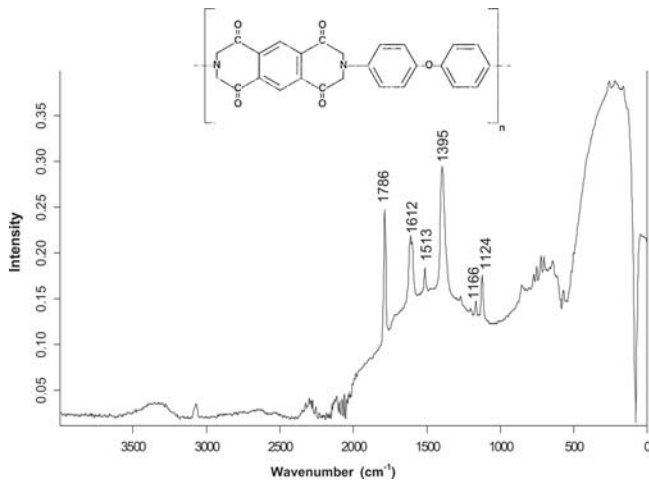


**Fig. 9** Raman spectrum for an unworn polyimide Vespel SP-1 sample, with characterization of absorption bands and functional groups in the molecular structure

bulk temperature. Fusaro (Ref 12) also observed two different regions, depending on the test conditions. The appearance of island and overall transfer regimes resembles spallation and brittle fracture, respectively. Fusaro also found transitions in friction mechanisms and attributed them to the higher polymer-chain mobility and orientation effects at the surface in absence of water. However, the mentioned orientation effects of the

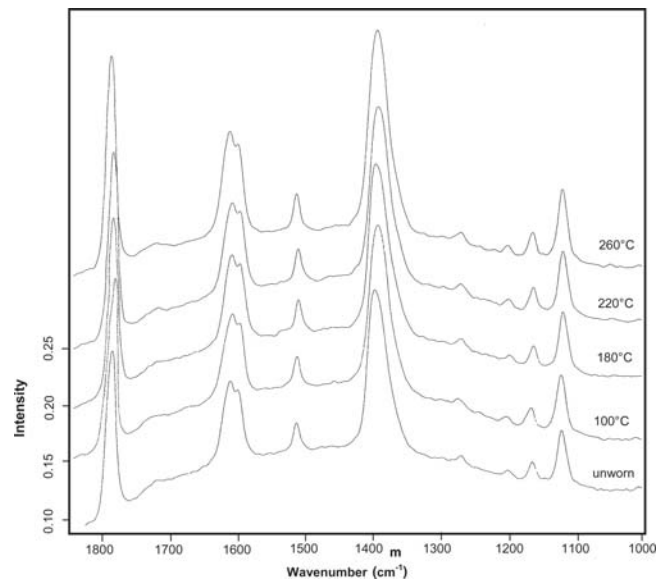


**Fig. 10** Details of Raman spectrum under sliding at 50 N and different bulk temperatures

polymer chains have not yet been illustrated and have not yet been correlated to the reorganization of the specific functional groups in the polyimide molecular structure. Therefore, they are discussed in more detail in the next section.

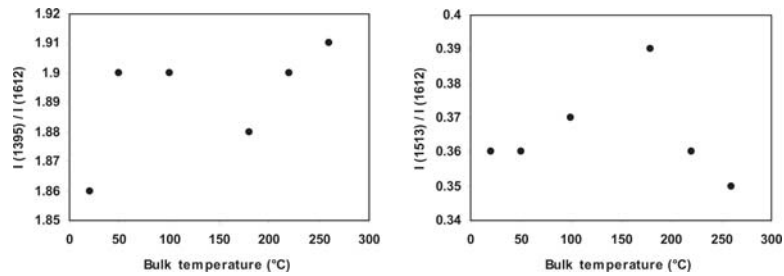


**Fig. 11** Evolution of the relative intensities of characteristic Raman bands as a function of the bulk temperature, measured on worn polyimide surfaces after sliding tests under 50 N

### 4.3 Fourier Transform Raman Spectroscopy of Worn Polyimide Surfaces

The Raman spectrum of an unworn Vespel SP-1 specimen is shown in Fig. 9 together with its molecular configuration. Characteristic polyimide absorption bands can be assigned to the C=C stretching vibration of the phenyl ring at 1612 and 1513  $\text{cm}^{-1}$  and the C-N stretching vibration of the imide system at 1395 and 1124  $\text{cm}^{-1}$ . The C=O stretching in the imide ring is characterized by a band at 1786  $\text{cm}^{-1}$ . Their identifications result from studies on the imidization process of polyimide (Ref 13), where the amide-related bands disappear and the corresponding imide-related bands appear as the bulk temperature increases. A theoretical study on the flexibility of different bonds in the polyimide PMDA-ODA structure was made by Walsh et al. (Ref 14).

Different spectra are taken from the polyimide sliding surfaces under 50 N normal load and bulk temperatures between 100 and 260 °C (Fig. 10). The spectra are analyzed by means of the baseline theory, where the change in relative intensity or frequency shift of certain peaks points toward creation, destruction, or reorientation of the related bond. The variation in relative intensity of some characteristic Raman bands is shown in Fig. 11. The 1612  $\text{cm}^{-1}$  peak is chosen as a reference band because it is correlated to the aromatic ring structure and has a central position in the spectrum. For quantitative analysis by Raman spectroscopy, the normalized percent relative intensities of absorption bands should be used to compensate for variations in experimental parameters, such as excitation intensity and sample positioning, factors that strongly affect the precision and detection limit values of Raman spectroscopy. The present 1612  $\text{cm}^{-1}$  reference band permits demonstration of the orientation of different functional groups relative to the phenyl ring in the imide structure. The normalized bands at 1513 and 1395  $\text{cm}^{-1}$  show opposite trends with discontinuities at 180 °C. They suggest a reorientation of the associated functional groups, depending on the sliding temperature. At 180 °C there occurs an orientation of the C=C bonding in the aromatic phenylene ring that may become tilted parallel to the sliding surface, represented by the maximum value in the 1513  $\text{cm}^{-1}$  band. At lower temperatures the movement of segments into the polymer chain seems to be restricted and do not allow for reorientation. At a higher temperature, thermally activated transitions may result in reorientation of several functional groups. It is also observed that, at 180 °C, the orientation of the C-N-C bonds is minimal. At higher temperatures, the latter functional group again becomes more stretched. The opposite orientation effects of both functional groups as presently observed under 180 °C can explain the maxima in friction and wear rate that

were measured for sliding under 50 N at 180 °C. Moreover, they are in accordance with the ability of polyimide transfer film formation at higher bulk temperatures.

## 5. Conclusions

The influence of a controlled bulk temperature between 100 and 260 °C on friction and wear of sintered polyimides (Vespel SP-1) was investigated herein for different normal loads and fixed sliding velocity. Transitions in both friction and wear are found in the region between 100 and 200 °C. It is observed that a polyimide transfer film onto the steel counterface develops only at temperatures above 180 °C. For the lowest test load (50 N), the wear rate has a maximum value at 180 °C in accordance with a peak value in friction.

By applying Raman spectroscopy on the worn polyimide surfaces, it is demonstrated that the transitions in both friction and wear can be related to orientation effects of the phenylene ring and C-N-C bonds. Characteristic absorption bands in the Raman spectrum show that both 1395 and 1513  $\text{cm}^{-1}$  bands are complementary for the reorientation effects at 180 °C. A maximum value for C=C orientation in the phenylene ring and a minimum orientation for the C-N-C imide bond explains the peak value observed in friction and wear at 180 °C.

## Acknowledgments

The authors are deeply grateful to Mr. Koen Peeters and Mr. Philippe Cantillon from Dupont du Nemours Belgium (Mechelen) who kindly supplied us with polyimide Vespel SP-1 cylindrical specimens. Optical microscopy was made possible by Ing. M. De Waele from the Belgian Welding Institute. This work was financially sponsored by FWO (Flemish Research Fund) and the Ghent University Research Board.

## References

1. Quadrant Engineering Plastic Products, *Delivery Programme*, ed. 1999-2000. Available at <http://www.quadrantep.com/products/datasheets.html>
2. R.L. Fusaro, Self-Lubricating Polymer Composites and Polymer Transfer Film Lubrication for Space Applications, *Tribol. Int.*, 1990, **23**(2), p 105-121
3. U.S. Tewari and J. Bijwe, Tribological Behaviour of Polyimides, *Polyimides: Fundamentals and Applications*, K.L. Mittal, M.K. Ghosh, Ed., Marcel Dekker Inc., (1996), p 533-583
4. K. Tanaka and T. Miyata, Studies on the Friction and Transfer of Semi-crystalline Polymers, *Wear*, 1977, **41**, p 383-398

5. T.W. Scharf and I.L. Singer, Monitoring Transfer Films and Friction Instabilities with in situ Raman Tribometry, *Tribol. Lett.*, 2003, **14**(1), p 3-8
6. T. Vankeirsbilck, Applications of Raman Spectroscopy in Pharmaceutical Analysis, *Trends Anal. Chem.*, 2002, **21**(12), p 869-877
7. Dupont de Nemours, *Vespel Parts and Shapes: Design Handbook*, 2002
8. H. Uetz and J. Wiedemeyer, *Tribologie der Polymere (Tribology of Polymers)*, Carl Hanser Verlag, Vienna, 1985, in German
9. E. Santner and H. Czichos, Tribology of Polymers, *Tribol. Int.*, 1989, **22**(2), p 103-109
10. K. Matsubara, M. Watanabe, and M. Karasawa, Frictional Properties of Irradiated Polymers at Elevated Temperatures, *Junkatsu (J. Jpn. Soc. Lubr. Eng.)*, 1969, **14**(43), p 99-103,
11. R.L. Fusaro, Effect of Atmosphere and Temperature on Wear, Friction and Transfer of Polyimide Films, *ASLE Trans.*, 1978, **21**(2), p 125-133
12. R.L. Fusaro, Polyimides: Tribological Use and Their Use as Lubricants, *Polyimides: Synthesis, Characterization and Applications*, K.L. Mittal, Ed., Plenum, New York, London, UK, 1984, p 2
13. K.H. Yy, Y.H. Yoo, J.M. Rhee, M.H. Lee, and S.C. Yu, Two-Dimensional Raman Correlation Spectroscopy of the Pathway for Thermal Imidization of Poly(amic acid), *Bull. Korean Chem. Soc.*, 2003, **24**(3), p 357-362
14. T.R. Walsh, C.G. Harkins, and A.P. Sutton, A Theoretical Study of Polyimide Flexibility, *J. Chem. Phys.*, 2000, **112**(9), p 4402-4412